Activity of a Two-Domain Antifreeze Protein Is Not Dependent on Linker Sequence

Nolan B. Holland,* Yoshiyuki Nishimiya,† Sakae Tsuda,† and Frank D. Sönnichsen*
*Department of Physiology and Biophysics, Case Western Reserve University, Cleveland, Ohio; and †Institute of Genome-Based Biofactory, National Institute of Advanced Industrial Science and Technology, Sapporo, Japan

ABSTRACT The reported NMR structure of RD3, a naturally occurring two-domain antifreeze protein, suggests that the two nearly identical domains are oriented to allow simultaneous binding of their active regions to the ice surface. It is implied that the nine residues linking the two domains play a role in this alignment, but this has not been established. We have designed and expressed a modified form of RD3 that replaces the nine-residue linker with a generic sequence of one serine and eight glycine residues to test the importance of the linker amino acid sequence. The modified linker is shown to have significantly different characteristics compared to the original linker. Heteronuclear nuclear Overhauser effect experiments show that the new linker residues have more mobility than the linker residues in the native protein. Further, NMR data show that the folding of the C-terminal domain is somewhat perturbed by the altered linker. Finally, distributions of residual dipolar couplings indicate that the two domains tumble and move independently of each other. Nevertheless, the thermal hysteresis activity of the modified protein is indistinguishable from that of native RD3, proving that increased activity of the two-domain antifreeze protein is not dependent on structure of the linker.

INTRODUCTION

Antifreeze proteins (AFPs) are a structurally diverse group of proteins. They have been isolated from a wide variety of organisms that are found in environments with ambient temperatures below the freezing point of water (1,2). These proteins are unique in their ability to reduce the effective freezing point of their aqueous solutions by an amount greater than would be expected by colligative freezing point depression. However, the melting temperature in AFP solutions remains colligatively determined. The difference between the freezing and melting temperatures is termed the thermal hysteresis and is the most common measure of AFP activity. Although these proteins have a wide variety of folding motifs and are classified into six types based on their structure, they all appear to function by binding to ice surfaces and kinetically inhibiting crystal growth.

Although the mechanism of the protein-ice binding has been researched for several decades, no unifying model has been established. It is the current thinking that surface complementarity between the binding region of an AFP and specific ice crystal planes leads to high affinity protein binding to the ice surface, as in receptor-ligand interactions (2). For a protein to match the ice crystal lattice, it has been observed that the protein binding regions tend to be relatively flat and slightly hydrophobic (1,3).

The structure-function relationship of AFPs has been probed by characterizing how structural differences among various native isoforms and artificially produced mutants affect the activity. Amino acid substitutions were used to determine the residues that make up the ice binding region in the globular Type III (4), the helical Type I (5), and insect (6) AFPs.

Repetitive AFPs, such as Type I AFP or AFGP, lend themselves to more systematic studies on scalable properties of ice binding. By observing the difference in activity in helical AFPs with different numbers of repeats, several groups demonstrated that in general, the larger the extent of the ice binding region the greater the activity. For example, Type I AFP is an α-helical protein formed from 11-residue repeat sequences, with the most common having three repeats. A naturally occurring isoform with four repeats is significantly more active (7). No Type I protein with less than three of the 11-residue repeats has been observed to have thermal hysteresis activity (8,9). Houston et al. did show that even though a single repeat peptide did not show thermal hysteresis activity, it did interact with ice by shaping the ice crystal (9). The effect of differing numbers of coils has also been investigated in the β-helical insect AFPs (10,11). Using a *Tenebrio molitor* AFP, Marshall et al. created isoforms which contained between six and eleven coils of twelve residue repeats (11). They showed that initially activity increased with length or added repeats. However, lengthening the protein beyond nine repeats led to decreases in activity, presumably due to accumulating steric mismatch with the ice crystal face.

For globular proteins, it would be difficult to increase the size of the binding region. However, it has been found that one AFP natively comprises two globular domains attached in tandem (12). The RD3 protein from the Antarctic eel pout consists of two nearly identical Type III domains connected

Submitted July 13, 2006, and accepted for publication September 18, 2006.

Address reprint requests to Frank D. Sönnichsen, Dept. of Physiology and Biophysics, Case Western Reserve University, 10900 Euclid Ave., Cleveland, OH 44106. Tel.: 216-368-5405; E-mail: fds@case.edu.

Nolan B. Holland's present address is Dept. of Chemical & Biomedical Engineering, Cleveland State University, 2121 Euclid Ave., Cleveland, OH 44115.

0006-3495/07/01/541/06 $2.00

doi: 10.1529/biophysj.106.091710

by a nine-residue linker. Using the same construction up to four Type III domains have been connected in series (13). The thermal hysteresis activity of RD3 at low concentrations has been reported to be as much as six times a single domain Type III protein (14). The three domain and four domain constructs have even greater activity than RD3 (13).

The reported structure of RD3, as determined by NMR, consists of the two domains oriented such that the binding faces are nearly coplanar, but rotated ~45° (14). It was suggested that this prealignment was important to the increased activity of the protein. The structure also suggested that if both domains bound simultaneously, they should be able to bind the crystal lattice with different orientations. Recently, a study, which artificially linked two Type III AFP domains, demonstrated that both domains must bind to the surface to be fully active (15).

To investigate the role of the linker on the activity of the protein, we have designed and expressed RD3-G, a mutant form of RD3, by replacing the nine-residue linker with one serine and eight glycine residues to increase the linker freedom and reduce the ability of the linker to induce prealignment. We demonstrate that the linker is flexible and that the domains likely diffuse independently, although the activity is indistinguishable from the native RD3.

MATERIALS AND METHODS

Construction of DNA encoding for RD3-G

We synthesized the genes encoding the amino terminal domain plus native linker (RD3Nl) (16) and the carboxy terminal domain (RD3C) of RD3, and utilized them as templates for the construction of DNA to encode RD3-G. A gene encoding RD3N plus part of the glycine-rich linker consisting of the amino acid sequence GGGGSGGG (denoted as RD3N-G) was prepared by polymerase chain reaction (PCR) utilizing i), a forward primer (5′-GAGCTGCAGTTAACTTTAAG-3′); ii), a reverse primer (5′-GCCGCCCCCAGACCCGCCACCGCCTTCGTAGTTTTTAACCATGTC-3′); and iii), our previously prepared gene encoding RD3Nl in pKK-223-3UC as a template. Likewise, the gene encoding a part of the glycine-rich linker sequence (GGGSGGGG) plus RD3C (denoted as G-RD3C) was amplified by using i), a forward primer (5′-CGGTGGCGGGTCTGGGGGCGGCGGTTCCGTTGTTGCTAACCAGCTG-3′); ii), a reverse primer (5′-GCTAGTTATTGCTCAGCGG-3′); and iii), the gene encoding RD3C in pET20b (Novagen). These prepared PCR products (DNA fragments of RD3N-G and G-RD3C) were combined by PCR. The recombination conditions were one cycle at 94°C (1 min), three cycles at 94°C (1 min), 54°C (1 min), and 72°C (2 min). The combined DNA fragment (denoted as RD3-G) was amplified by using a forward primer (5′-GAGCTGCAGTTAACTTTAAG-3′) and a reverse primer (5′-GCTAGTTATTGCTCAGCGG-3′). The purified DNA fragment of RD3-G and pET20b (Novagen) were digested with *Nde*I and *Bam*HI restriction endonucleases, and ligated using T4 DNA ligase.

Expressions and purifications of the recombinant multimers

The plasmid DNA was transformed into *Escherichia coli* strain BL 21 (DE3), which were grown at 28°C in LB medium supplemented with ampicillin (100 μM) until the cell growth reached the early stationary phase. To induce the expression of RD3-G, 0.5 mM of IPTG was added and the cultures were grown at 28°C overnight. The purification of RD3-G was performed as previously described (14). The culture medium was centrifuged at 4000 $\times$ g for 30 min at 4°C, and the precipitated cell pellet containing the inclusion body of RD3-G sonicated. After the sonication, RD3-G was collected by centrifugation at 12,000 $\times$ g for 30 min at 4°C. The precipitant was washed with 0.1% (v/v) Triton X-100, 1 mM EDTA three times, and dissolved into 100 mM Tris-HCl (pH 8.5) containing 6 M guanidine hydrochloride at room temperature. The dissolved RD3-G was diluted with 50 mM K_2PO_4 containing 100 mM NaCl (pH 10.7) at 4°C, followed by extensive dialysis against 50 mM sodium acetate (pH 3.7) at 4°C. The precipitant formed during dialysis was removed occasionally by centrifugation. The supernatant containing AFP was loaded onto a high-S column (BIO-RAD), and the column-bound AFP was eluted with a linear NaCl gradient (0–0.5 M) using 50 mM sodium acetate buffer (pH 3.7). The fractions containing the isolated AFP were stored and dialyzed against 0.1 M ammonium bicarbonate (pH 7.9). The purity and the molecular weights (14 kDa) of the samples were checked by 16% SDS-PAGE.

NMR spectroscopy

A protein solution for NMR experiments was prepared from purified RD3-G to a concentration of 0.9 mM in 50 mM potassium phosphate (pH 6.8) with 10% D_2O (v/v) and 2 mM sodium azide. For comparison, a solution of RD3 was prepared in the same buffer. These samples were stored at 5°C. NMR spectra were obtained using Varian INOVA 500 and 600 MHz spectrometers. Two-dimensional ^{15}N HSQC spectra were obtained at 4° and 25°C. These spectra are compared to previously reported and assigned HSQC spectra of RD3 (16,17). Before and after each set of experiments ^{15}N HSQC were measured to ensure that no significant changes occurred to the protein sample.

^{15}N heteronuclear NOE relaxation data was collected with the 500 MHz spectrometer at 4°C. The two spectra, nuclear Overhauser effect (NOE) and NoNOE were acquired in succession with a repetition delay of 5.0 s, and saturation periods of 3.0 and 0.0 s, respectively. Spectra were obtained with 120 increments and 32 scans, and spectral widths of 6600 and 1650 Hz for ^{1}H and ^{15}N, respectively. NOE ratios were obtained as the peak intensity ratio of NOE/NoNOE resonances, with errors based on spectral noise.

A solution sample for residual dipolar coupling measurements was prepared by adding 75 μl of 51 mg/ml Pf1 filamentous phage (Profos, Regensburg, Germany) to 200 μl of the RD3-G protein solution resulting in phage at a concentration of 14 mg/ml. This concentration was sufficient to partially align the protein resulting in measurable residual dipolar couplings. Spectra for obtaining the RDC measurements were performed with the 600 MHz spectrometer at 4°C. Two different transverse relaxation-optimized spectroscopy (TROSY) experiments were utilized to obtain the two ^{1}H upfield components of the ^{1}H–^{15}N multiplet (18). The ^{1}H–^{15}N coupling is measured from the separation of the ^{15}N downfield (TROSY) and upfield components. For both solutions with and without phage, the two spectra were obtained sequentially using identical spectrometer parameters, except for the number of transients. Since the ^{15}N upfield component expectedly was somewhat broader, more transients were required to get an adequate signal to noise ratio comparable to the standard TROSY peak. Data consisting of 180 increments of 512 complex points were collected for each experiment with spectral widths of 6600 and 1650 Hz for the ^{1}H and ^{15}N dimensions, respectively.

All spectra were identically processed through NMRPipe and analyzed in NMRView. The peaks were labeled for each spectrum based on shifted values from the reported assignments of RD3. (17). The ^{1}H–^{15}N coupling was measured for each peak in both the aligned and unaligned samples. The differences in peak separations between the two samples were taken to be the residual dipolar couplings.

Activity measurements

Activity measurements were performed for the purified protein dissolved in 0.1 M ammonium bicarbonate (pH 7.9) using a nanoliter osmometer (model OM 802, Vogel, Giessen, Germany). The freezing point determinations were performed using a Leica DMLB 100 photomicroscope (Wetzlar,

Germany) equipped with a Linkam LK600 temperature controller (Waterfield, UK) and charge-coupled device camera. Three measurements of the freezing (T_f) and melting (T_m) temperatures were obtained using fresh samples at each concentration. Averaged values of the difference between T_f and T_m were used for determination of the thermal hysteresis activity.

RESULTS

NMR spectroscopy was used to compare the structural and dynamic properties of the modified AFP RD3-G to the native two-domain protein RD3, which has previously been assigned and characterized (16,17). RD3 is comprised of two small, nearly identical Type III AFP globular domains. Their structure is described by a compact β-sheet fold (19,20), which also has been named pretzel fold (21). The sequence similarity between the two domains is 84%. In the wild-type RD3, the two domains are separated by a nine-residue linker sequence (DGTTSPGLK), which was replaced in this study with a glycine rich sequence (GGGGSGGGG) making the RD3-G mutant. The dispersion of peaks in the HSQC NMR spectra of RD3-G suggests that the protein is well folded. In comparing the spectrum with that of native RD3, the similarity in the positions and relative intensities of peaks is clear (Fig. 1). One obvious difference is that new peaks corresponding to the glycines of the modified linker appear. These are clustered around 109 ppm and 8.3 ppm for the ^{15}N and ^{1}H chemical shifts, respectively. Additionally, the peaks from the replaced linker residues are no longer present. The ^{15}N chemical shift for a random coil glycine preceded by another glycine is expected to be at 108.7 ppm, whereas it should be slightly higher when preceded by glutamic acid (108.9 ppm) or serine (109.9 ppm); the ^{1}H chemical shifts are 8.41, 8.56, and 8.57 ppm when preceded by glycine, glutamic acid, and serine, respectively (22).

A second observation is that a small number of peaks shifted compared to RD3. Excluding the linker, chemical shifts for 20 residues differ by at least 15 Hz versus native RD3. Closer examination reveals that 16 of these chemical shift changes are for residues in the carboxy terminal domain, whereas the remaining four (residues E36, N62, Y63, and E64) are in close spatial proximity to the linker in the amino-terminal domain. This suggests that the changes in the linker somewhat perturbed the folding of the carboxy terminal domain while leaving the amino-terminal domain relatively unchanged. However, since most of the shifts are relatively small and none of the ice binding residues is affected (Fig. 2), it suggests that the overall fold and stability of the protein is not significantly altered.

Further evidence of the glycine-rich linker affecting the folding of the carboxy terminal domain is a slow spectral change observed when the protein sample is warmed. When the solution temperature was increased to 25°C, peaks from residues in the second domain slowly lost intensity over several hours, and other peaks (previously unobserved) began to appear. The intensity of peaks from the amino terminal domain remained constant throughout. In contrast, the spectra of native RD3 are stable at 25°C. It is unknown what the nature of the second state is (it may be a second stably folded conformation, a molten globule, or fully unfolded domain),

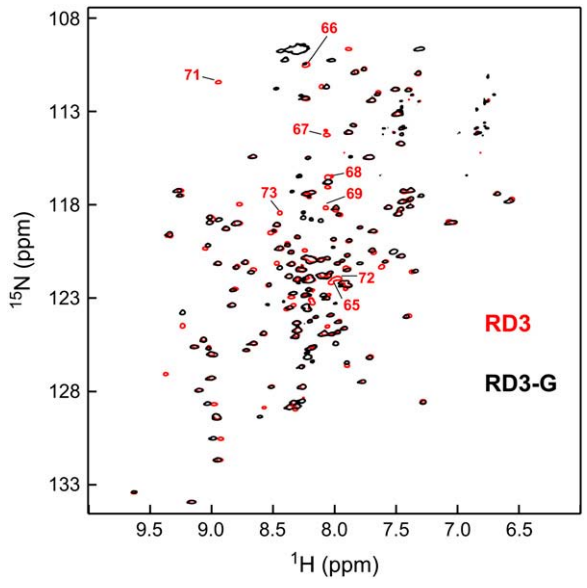

FIGURE 1 RD3-G ^{1}H,^{15}N-HSQC spectrum (*black*) overlaying that of RD3 (*red*). Experiments were performed at 4°C and pH 6.8. The peak positions are nearly identical for both proteins with the exception of the cluster of peaks observed around 109 ppm ^{15}N and 8.5 ppm ^{1}H. These originate from the glycine residues that replace the residues of the native linker, which are labeled by residue number.

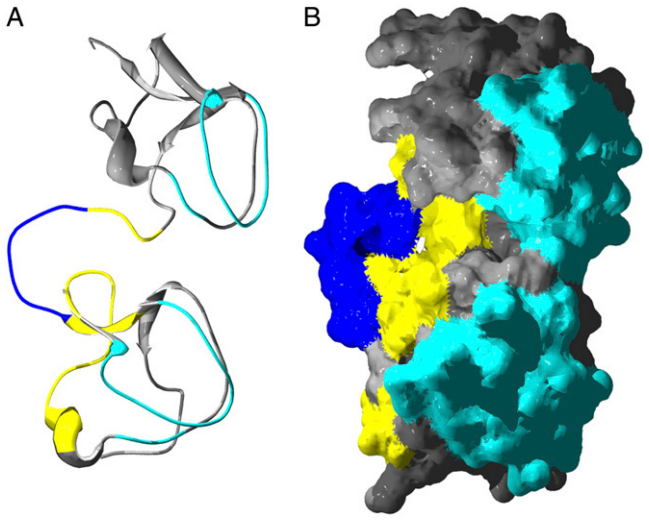

FIGURE 2 RD3-G structures based on the solution structure of RD3 (PDB 1C8A) in (*A*) backbone and (*B*) surface representations. The linker region is colored blue and the ice-binding face is turquoise. Resonance frequencies of residues that are shifted by at least 15 Hz (greater than half the peak width) from the corresponding peak in RD3 are colored yellow. All but four of these residues are in the carboxy terminal domain, and none are residues that comprise the ice binding face. Side chains are only shown for the highlighted residues, and no protons are displayed. Prepared with SPDB Viewer 3.7 and rendered with POV-Ray.

but the conversion appears to be reversible upon lowering the temperature. Characterization of this structure is beyond the focus of this study since it occurs at nonphysiological temperatures high above solution freezing points.

Thermal hysteresis measurements of RD3-G corroborate the NMR data that suggests that the protein is folded properly. These measurements demonstrate that replacing the native linker with the glycine linker does not alter the activity of the protein. Fig. 3 shows a direct comparison between the thermal hysteresis of native RD3 and that of RD3-G at concentrations up to 0.3 mM.

Dynamics of the protein backbone were characterized using heteronuclear NOE relaxation measurements. A ratio of 1.0 indicates that there is no mobility of the N-H bond, and the lower the ratio, the greater the mobility of the bond. Simple Brownian tumbling of a well-folded protein will result in NOE ratios of ~0.7 for 500 MHz field strength. Portions of a protein that can move independently, such as terminal residues, will have lower ratios. Measurements were made for each residue with a backbone NH. The NOE ratios for the domains of RD3-G and native RD3 (Fig. 4) fall within the expected range for a well-folded protein; however, the linker regions are significantly lower. Since no specific assignment was achieved for the spectral peaks corresponding to the new glycine residues in the linker, the eight glycine peaks were ordered such that the NOE ratios were a minimum in the middle of the linker, similar to native RD3. It is stressed that this may not be the correct assignment, but that in comparison to the native linker, it is the most plausible assignment. In any case, these data reveal that the backbone of the linker region is relatively flexible compared to the well-folded domains. Further comparing the NOE ratios of the native linker and the glycine-rich linker, it is also observed that the latter is more flexible as judged by the significantly lower NOE ratios. As the glycines have no significant side chains to impede chain motion this additional flexibility is expected.

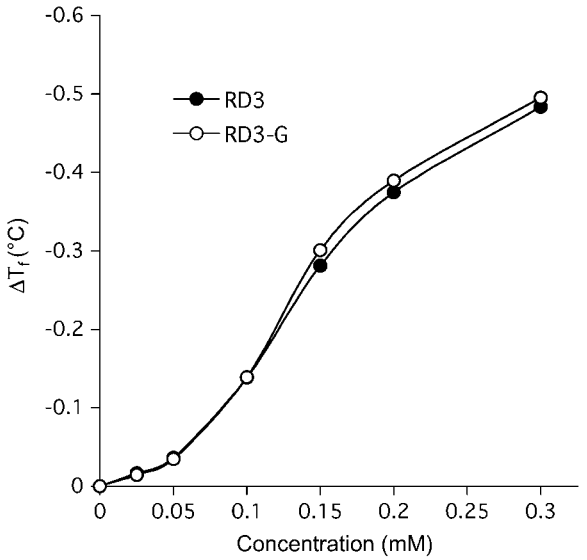

FIGURE 3 Thermal hysteresis activity of RD3 and RD3-G.

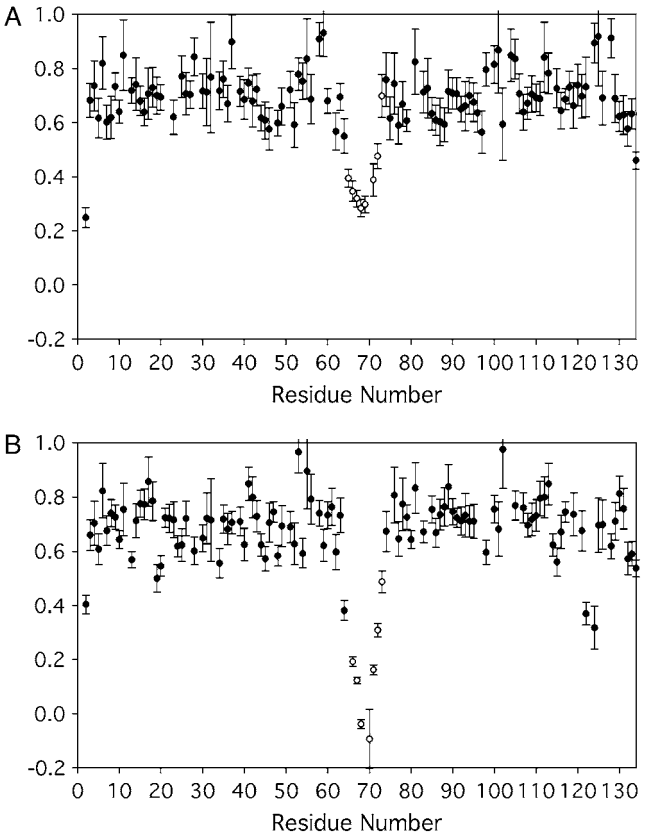

FIGURE 4 ^{15}N heteronuclear NOE relaxation data for (*A*) RD3 and (*B*) RD3-G. The NOE ratios are plotted against the residue number, with the linker residues as open circles. For residues in a stably folded protein the value should be ~0.7. The lower the value the more mobility the residue has. The low values for the linker region in both RD3 and RD3-G indicate that the linker is relatively flexible and unstructured. Additionally, the glycine-rich linker of the RD3-G has significantly lower ratios indicating that it is more flexible than the native linker of RD3.

Residual dipolar couplings were measured for 61 residues, 35 in the amino terminal domain and 26 in the carboxy terminal domain. RDCs for many residues could not be determined because of the significant overlap of the peaks of the two domains. Resonance overlap also made it impossible to obtain RDCs for the linker region. The RDC values are plotted in Fig. 5 against the residue number. It is evident from this plot that the distribution of RDCs is different for the two domains. Firstly, equivalent residues or positions in the amino and carboxy terminal domains exhibit largely differing RDC values, which suggest differing orientations of the domains with respect to the alignment tensor. Secondly, the carboxy terminal domain has a narrower distribution centered at a higher value than the amino terminal domain. The distribution of RDCs depends primarily on the degree and symmetry of the protein alignment. For a protein that aligns as a single unit, the RDCs should fall within a single

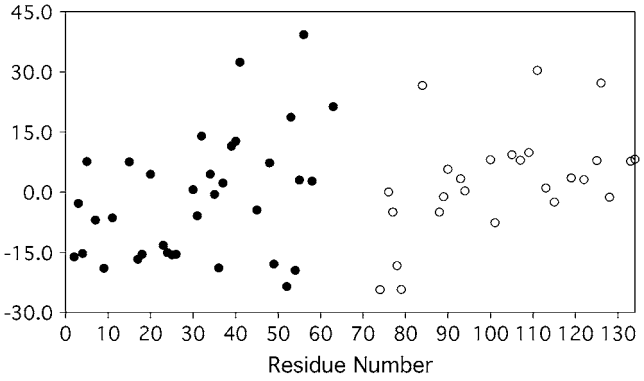

FIGURE 5 A plot of residual dipolar couplings (RDCs) of RD3-G that is slightly aligned in a filamentous phage solution. The RDCs are plotted against the residue numbers illustrating the difference in the distribution of values between the amino terminal domain (*solid circles*) and carboxy terminal domain (*open circles*).

distribution. If two regions of the protein can move independent of each other, however, they can align independently which may result in two distinct RDC distributions. Thus, the present observation of different RDC distributions here is indicative of an independent movement of the two domains.

DISCUSSION

This set of experiments on the modified RD3 antifreeze protein was performed to help elucidate the origin of the hyperactivity of the two-domain Type III antifreeze protein. The multimerization of the type III domains, as reported by Nishimiya et al., demonstrates that increased numbers of domains leads to increased activity, at least up to a certain point (13).

Some light was shed on the mechanism through which an extra domain leads to enhanced activity through elegant experiments performed by Baardsnes et al. (15). Using an isoform of Type III AFP different from RD3, two identical domains were connected using the RD3 linker motif. This construction showed two times the activity compared to the single domain protein. When one of the two domains is inactivated by point mutations, the activity of the protein is reduced to only 1.2 times that of the single domain AFP. This indicates the greater size of the protein, independent of the extra binding region, cannot account for the entire increase in activity. An additional construct was prepared where two domains were connected through a disulfide bond between cysteine residues engineered into the C-terminal end of the proteins, far from the binding region. This leaves both of the active binding regions free to interact with the ice surface, but restricts their mobility thereby preventing both domains from binding simultaneously. Again, this led to a reduction in activity to only 1.2 times that of a single domain Type III AFP. It is concluded that simultaneous binding of the two domains is necessary to generate the full increase in activity, presumably by doubling the binding site area.

Since it has been demonstrated that having two active domains that can simultaneously bind to the ice surface is important in producing the activity of RD3, this raises the question as to whether the domains actually behave as a single binding face (a simple doubling of the binding site area), or whether it is better described as two independent binding domains which are simply confined to a certain distance from each other by the linker. This makes a difference in the theoretical treatment of the ice-protein interaction. If the domains act as a single binding entity, the doubling of the binding area should increase the binding affinity of the protein, as for repetitive type proteins with additional repeats. However, if they bind independently, binding affinity for each domain would remain the same as the single domain protein, but since there are two binding regions, the avidity would increase. Once one domain is bound, the second domain is confined to a small region near the surface leading to an increased effective concentration, increasing the probability of binding and decreasing the probability of the entire protein from desorbing.

If the domains behave as a single binding face, some structural component must orient them so that they bind as one unit. The reported structure of RD3 determined by NMR suggests that the domains are aligned (14). The binding faces are coplanar, but rotated close to 45° to each other. If RD3 binds to the ice crystal with this orientation, it implies that the binding region could interact with an ice plane with a different orientation. This is a remarkable claim, since it has been suggested that the binding region has high specificity for a specific orientation on the ice surface, and the ice crystal lattice is chiral. If both domains bind to the same ice plane, it would be expected that the domains bind with the same orientation on the crystal lattice.

Our data are the first to show two Type III domains connected by a nonnative linker resulting in the same thermal hysteresis activity as the native RD3 protein. In previous experiments, only domains connected with the native linker successfully reproduced the hyperactivity of native RD3. Since there is no decreased activity with the new linker, any structuring based on linker composition is not responsible for holding the domains in a specific configuration. This is reasonable since the NOE relaxation data further shows that the native linker is relatively flexible and also unlikely to be structured. If the linker were not structurally capable of independently constraining the domains, other interactions such as interdomain contacts would be necessary for domain prealignment. Several interdomain NOEs were observed in RD3 resulting in calculated structures with domain-prealignment (14). An alternative interpretation may be that the NOEs are the result of weak or transient interactions instead of strong interactions that lead to the prealignment of the domains. Our data cannot exclude either of these interpretations. Furthermore, RD3 and RD3-G possibly differ in these contacts, as supported by the subtle chemical shift differences between these proteins (Fig. 1). Complete assignments of RD3-G, further experiments, and a full comparison of data of both proteins will be required to determine whether these interactions are present and comparable in RD3-G and RD3.

The residual dipolar coupling data for RD3-G suggest that the prealignment, if it occurs at all, is not a rigid alignment. The domains are to some extent able to align independently, and this could suggest that the domains are able to freely sample all the conformational space made accessible by the flexible linker. Since RD3-G is less confined by its linker, yet has the same thermal hysteresis as RD3, this questions the previous conclusion that RD3 prealignment is responsible for its increased activity. We suggest that even in the presence of a more restricting linker, prealignment may not play a significant role in the protein activity. In other words, the increased activity of the two-domain antifreeze proteins may be due primarily to an increase in avidity and not an increase in affinity for the ice surface. This is clearly different than the mechanism observed from other experiments where activity of helical AFPs was increased or decreased by respectively adding or removing residues (7–11). In those constructs it is a clear change in the area of binding that corresponds to changes in affinity. This may explain why the relative increase in thermal hysteresis for RD3 compared to single domain AFP diminishes at high concentrations and plateaus at maximal hysteresis values identical to those of equivalent monomeric domains. In contrast, maximum hysteresis remains significantly different even at high concentrations if one compares helical proteins with differing number of repeats or coils.

CONCLUSIONS

We have successfully replaced the nine residue linker connecting the two nearly identical domains of the RD3 antifreeze protein with a glycine rich linker. The linker has significantly more backbone flexibility than the native linker, as measured by heteronuclear NOE relaxation experiments. Measurement of RDCs suggest that the domains have significant degree of independence. Nevertheless, the modified linker does not alter antifreeze functional activity of the protein. The reported prealignment of native RD3 domains as determined by solution NMR does not appear necessary for the heightened activity of RD3. This casts doubt as to whether the two RD3 domains are strongly prealigned, and how much this influences the resulting activity. Only a conclusive study of the domain alignment of native RD3 will answer these questions.

The authors thank the Cleveland Center for Structural Biology for use of their spectrometer facilities and to Dale Ray for spectrometer upkeep.

This work was supported by the National Institutes of Health (DK07678, GM55326, and DK57306).

REFERENCES

1. Davies, P. L., J. Baardsnes, M. J. Kuiper, and V. K. Walker. 2002. Structure and function of antifreeze proteins. *Philos. Trans. R. Soc. Lond. B Biol. Sci.* 357:927–933.
2. Jia, Z. C., and P. L. Davies. 2002. Antifreeze proteins: an unusual receptor-ligand interaction. *Trends Biochem. Sci.* 27:101–106.
3. Sönnichsen, F. D., C. I. DeLuca, P. L. Davies, and B. D. Sykes. 1996. Refined solution structure of type III antifreeze protein: hydrophobic groups may be involved in the energetics of the protein-ice interaction. *Structure.* 4:1325–1337.
4. Chao, H., F. D. Sönnichsen, C. I. Deluca, B. D. Sykes, and P. L. Davies. 1994. Structure-function relationship in the globular type-III antifreeze protein—Identification of a cluster of surface residues required for binding to ice. *Protein Sci.* 3:1760–1769.
5. Baardsnes, J., L. H. Kondejewski, R. S. Hodges, H. Chao, C. Kay, and P. L. Davies. 1999. New ice-binding face for type I antifreeze protein. *FEBS Lett.* 463:87–91.
6. Marshall, C. B., M. E. Daley, L. A. Graham, B. D. Sykes, and P. L. Davies. 2002. Identification of the ice-binding face of antifreeze protein from *Tenebrio molitor*. *FEBS Lett.* 529:261–267.
7. Chao, H., R. S. Hodges, C. M. Kay, S. Y. Gauthier, and P. L. Davies. 1996. A natural variant of type I antifreeze protein with four ice-binding repeats is a particularly potent antifreeze. *Protein Sci.* 5:1150–1156.
8. Harding, M. M., L. G. Ward, and A. D. J. Haymet. 1999. Type I 'antifreeze' proteins—Structure-activity studies and mechanisms of ice growth inhibition. *Eur. J. Biochem.* 264:653–665.
9. Houston, M. E., H. Chao, R. S. Hodges, B. D. Sykes, C. M. Kay, F. D. Sönnichsen, M. C. Loewen, and P. L. Davies. 1998. Binding of an oligopeptide to a specific plane of ice. *J. Biol. Chem.* 273:11714–11718.
10. Leinala, E. K., P. L. Davies, D. Doucet, M. G. Tyshenko, V. K. Walker, and Z. C. Jia. 2002. A beta-helical antifreeze protein isoform with increased activity—Structural and functional insights. *J. Biol. Chem.* 277:33349–33352.
11. Marshall, C. B., M. E. Daley, B. D. Sykes, and P. L. Davies. 2004. Enhancing the activity of a beta-helical antifreeze protein by the engineered addition of coils. *Biochemistry.* 43:11637–11646.
12. Wang, X., A. L. Devries, and C. H. C. Cheng. 1995. Antifreeze peptide heterogeneity in an antarctic eel pout includes an unusually large major variant comprised of 2 7-KDa type-III AFPs linked in tandem. *Biochim. Biophys. Acta.* 1247:163–172.
13. Nishimiya, Y., S. Ohgiya, and S. Tsuda. 2003. Artificial multimers of the type III antifreeze protein— Effects on thermal hysteresis and ice crystal morphology. *J. Biol. Chem.* 278:32307–32312.
14. Miura, K., S. Ohgiya, T. Hoshino, N. Nemoto, T. Suetake, A. Miura, L. Spyracopoulos, H. Kondo, and S. Tsuda. 2001. NMR analysis of type III antifreeze protein intramolecular dimer—Structural basis for enhanced activity. *J. Biol. Chem.* 276:1304–1310.
15. Baardsnes, J., M. J. Kuiper, and P. L. Davies. 2003. Antifreeze protein dimer—When two ice-binding faces are better than one. *J. Biol. Chem.* 278:38942–38947.
16. Miura, K., S. Ohgiya, T. Hoshino, N. Nemoto, M. Odaira, K. Nitta, and S. Tsuda. 1999. Determination of the solution structure of the N-domain plus linker of antarctic eel pout antifreeze protein RD3. *J. Biochem. (Tokyo).* 126:387–394.
17. Miura, K., S. Ohgiya, T. Hoshino, N. Nemoto, K. Nitta, and S. Tsuda. 2000. Assignments of H-1, C-13, and N-15 resonances of intramolecular dimer antifreeze protein RD3. *J. Biomol. NMR.* 16:273–274.
18. Weigelt, J. 1998. Single scan, sensitivity- and gradient-enhanced TROSY for multidimensional NMR experiments. *J. Am. Chem. Soc.* 120:10778–10779.
19. Sönnichsen, F. D., B. D. Sykes, H. Chao, and P. L. Davies. 1993. The nonhelical structure of antifreeze protein type-III. *Science.* 259:1154–1157.
20. Jia, Z. C., C. I. DeLuca, H. M. Chao, and P. L. Davies. 1996. Structural basis for the binding of a globular antifreeze protein to ice. *Nature.* 384:285–288.
21. Yang, D. S. C., W. C. Hon, S. Bubanko, Y. Q. Xue, J. Seetharaman, C. L. Hew, and F. Sicheri. 1998. Identification of the ice-binding surface on a type III antifreeze protein with a ''Flatness function'' algorithm. *Biophys. J.* 74:2142–2151.
22. Schwarzinger, S., G. J. A. Kroon, T. R. Foss, J. Chung, P. E. Wright, and H. J. Dyson. 2001. Sequence-dependent correction of random coil NMR chemical shifts. *J. Am. Chem. Soc.* 123:2970–2978.